Boundary Condition Expansion of Basis Functions Method Implemented by Fast Fourier Transform Algorithms

LJUBIŠA STANKOVIĆ AND SVETOZAR JOVIĆEVIĆ

Abstract—**This paper presents a new approach to boundary value problems. It is based on boundary condition expansion on basis functions. The expansion coefficients are determined using the fast Fourier transform of basis functions on the boundary. This approach is compared with the least-squares boundary residual method (LSBRM). It is shown that this approach results in a considerable reduction in computation time in comparison with the original LSBRM. The procedure is successfully demonstrated on diffraction and eigenvalue problems.**

I. Introduction

METHODS of modal expansion have frequently been used in solving electromagnetic boundary value problems. Among them the point matching method [1] is one of the oldest and simplest mathematical methods of determining expansion coefficients. It has been used in solving eigenvalue problems [2], [3] and in the solution of the problems of scattering from a periodic surface [4], [5]. The least-squares boundary residual method (LSBRM), an improved point matching method, has been introduced in scattering problems [6] and has also been successfully used both in solving eigenvalue problems and dielectric waveguides [7], [8] and in acoustic wave propagation along periodic gratings [9].

The applicability of the LSBRM method has been demonstrated in electrostatic and eddy currents and also in the treatment of nonharmonic field problems [10], [11]. The method has made possible a very effective analysis of waveguides with complex cross sections [12]. In all of these problems the least-squares boundary residual method has been found to be very accurate and convenient. It is therefore recommended not only in the specific area of microwave techniques, but also as a reliable numerical procedure of more general interest in the solution of boundary value problems. Although the boundary conditions can be satisfied on certain parts of the boundary through an appropriate choice of basis functions, the numerical integration of basis function products along the rest of the boundary is a formidable procedure. Efforts in reducing the computation time seem to be worthwhile. The transformation of basis functions into rectangular pulse functions [13] is a possible technique. This paper presents an approach to solving boundary value problems using the fast Fourier transforms (FFT) of basis functions along the boundary, resulting in a reduction in computation time.

Manuscript received May 28, 1988; revised September 22, 1989.

The authors are with the Electrical Engineering Department, University of Titograd, 81000 Titograd, Yugoslavia.

IEEE Log Number 8932991.

II. Theory

Let us consider a two-dimensional equation of the Helmholtz type:

$$\frac{\partial^2 u}{\partial x^2} + \frac{\partial^2 u}{\partial y^2} + k^2 u = 0 \tag{1}$$

with boundary condition along the line $L = L_1 \cup L_2$ defined by the function $l(x)$. The boundary condition on L_1 is of the Dirichlet type and on L_2 of the Neumann type:

$$g(x) = \begin{cases} u(x, l(x)) & \text{on } L_1 \\ \dfrac{\partial u(x, l(x))}{\partial n} & \text{on } L_2. \end{cases} \tag{2}$$

A solution to (1) with boundary condition (2) will be sought as a sum of basis functions $\varphi_m(x, y)$ of (1):

$$u(x, y) = \sum_{m=1}^{M} c_m \varphi_m(x, y). \tag{3}$$

Let us define the functions $f_m(x)$ as

$$f_m(x) = \begin{cases} \varphi_m(x, l(x)) & \text{on } L_1 \\ k_n \dfrac{\partial \varphi_m(x, l(x))}{\partial n} & \text{on } L_2 \end{cases} \tag{4}$$

taking k_n as weighting factor for Neumann's boundary condition. If functions $f_m(x)$ can be developed in Fourier series, then we can express them in the form

$$f_m(x) = \sum_{\nu=-N/2}^{N/2-1} F_m(\nu) e^{j(2\pi/a)\nu x} \tag{5}$$

where a denotes the length of periodicity along the x axis. If the functions $f_m(x)$ are band-limited, we can obtain the coefficients $F_m(\nu)$ from the samples of functions $f_m(x)$ at the points $x = an/N$ using the FFT algorithms (see [14]). Therefore,

$$F_m(\nu) = \mathrm{FFT}\{f_m(n)\} \tag{6}$$

where $f_m(n) = f_m(x)_{|x=(a/N)n}$ denotes the nth sample of the mth basis function on the boundary.

It should be pointed out that in many electromagnetic problems only one of the types of boundary conditions given by (2) is prescribed along the boundary line. However, in the problems where one of the types of boundary conditions is given on one part of the boundary line L and the other type on the remaining part of the boundary, functions $f_m(x)$ and $g(x)$ may have a discontinuity of the first kind. But even this does not affect the possibility of developing functions in Fourier series, although it does affect the convergence. Such problems were analyzed in [24].

The deviation from the boundary value is

$$e(x) = \sum_{m=1}^{M} c_m f_m(x, l(x)) - g(x). \tag{7}$$

With $F_g(\nu)$ denoting the FFT of the boundary condition:

$$F_g(\nu) = \mathrm{FFT}\{g(n)\} \tag{8}$$

and after interchanging the order of summation, the error in any point can be written as

$$e(x) = \sum_{\nu=-N/2}^{N/2-1} \left[\sum_{m=1}^{M} c_m F_m(\nu) - F_g(\nu) \right] e^{j(2\pi/a)\nu x}. \tag{9}$$

Now, if $M = N$ then the unknown coefficients c_m can be found by taking all amplitudes to be equal to zero, i.e., from the system

$$\begin{Vmatrix} F_1(-M/2) & \cdots & F_M(-M/2) \\ \vdots & & \\ F_1(M/2-1) & \cdots & F_M(M/2-1) \end{Vmatrix} \begin{Vmatrix} c_1 \\ \vdots \\ c_M \end{Vmatrix} = \begin{Vmatrix} F_g(-M/2) \\ \vdots \\ F_g(M/2-1) \end{Vmatrix}. \tag{10}$$

Accepting that $M = N$, i.e., that the number of expansion coefficients is equal to the number of basis function samples, we actually come to a variant of the collocation method. However, this procedure has an advantage over the standard collocation procedure in that the values of coefficients $F_m(\nu)$ differ more from one another than the values of the basis functions themselves. Therefore matrix (10) is not ill-conditioned. Still, the size of system (10) acts as a serious disadvantage, as is the case in the original procedure of the collocation method. However, not all N samples need to be taken, only the first M ($M < N$) harmonics, i.e., the number of modes in (3), so that we obtain a very much reduced system of order M.

In [15] we minimized the mean of the absolute square value of the error (7), which, knowing that it was equal to the sum of the mean square values of all harmonics:

$$\overline{|e(x)|}^2 = \sum_{\nu=-N/2}^{N/2-1} \left[\sum_{m=1}^{M} c_m F_m(\nu) - F_g(\nu) \right] \cdot \left[\sum_{m=1}^{M} c_m^* F_m^*(\nu) - F_g^*(\nu) \right] \tag{11}$$

gave a system with unknown expansion coefficients:

$$\begin{Vmatrix} A_{11} & \cdots & A_{1M} \\ \vdots & & \\ A_{M1} & \cdots & A_{MM} \end{Vmatrix} \begin{Vmatrix} c_1 \\ \vdots \\ c_M \end{Vmatrix} = \begin{Vmatrix} B_1 \\ \vdots \\ B_M \end{Vmatrix} \tag{12}$$

where A_{ml} and B_m denote

$$A_{ml} = \sum_{\nu=-N/2}^{N/2-1} F_l(\nu) F_m^*(\nu)$$

$$B_m = \sum_{\nu=-N/2}^{N/2-1} F_g(\nu) F_m^*(\nu). \tag{13}$$

In treating both procedures (10) and (12) as variants of the general moment method (see [23]), a correspondence is found. The requirements $e(x) = 0$ can be written in the form

$$\sum_{m=1}^{M} c_m f_m(x) = g(x). \tag{14}$$

If we take, as a weighting function, the complex conjugate of only one basis function's harmonic, i.e., $F_m^*(\nu)\exp(-2\pi x\nu/a)$, from (14) after dividing by $F_m^*(\nu)$ and integrating within the interval $(0, a)$, we get system (10).

On the other hand, if we take the complex conjugate of the basis function along the boundary, i.e., $f_l^*(x)$, as a weighting function, we obtain the following system:

$$\sum_{m=1}^{M} c_m (f_m, f_l^*) = (g, f_l^*), \qquad l = 1, 2, \cdots, M \tag{15}$$

where (f_m, f_l^*) is a scalar product along the interval $(0, a)$. System (15) is equivalent to the requirement $\overline{|e(x)|}^2 = 0$. By introducing the FFT of functions $f_m(x)$, $f_l(x)$, and $g(x)$ into (15) and with the orthogonality of harmonics, we obtain system (12).

Thus, we can conclude that system (12) is more general since it includes the complete Fourier transform (FT) of the weighting functions and that (10) is a special case. By including only one harmonic and assuming the same order, system (12) will produce greater accuracy than (10) but with a greater computation time.

In order to achieve more accurate results the integration interval in (15) should be divided into a greater number of subintervals; i.e., a greater number of function samples and FFT harmonics should be taken. However, in sum (13) it is possible to take only N_1 most significant modes. In accordance with our previous discussion this means to take as a weighting function the N_1 harmonics of the basis

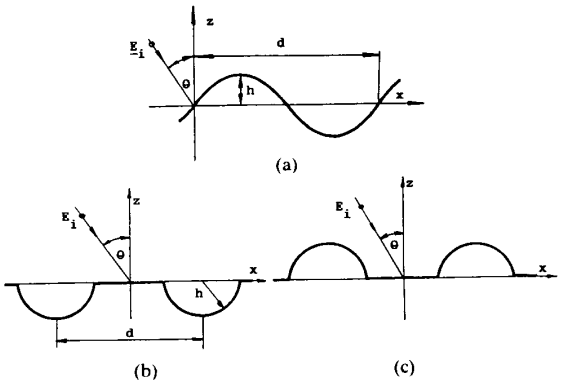

Fig. 1. The grating of (a) sinusoidal, (b) semicircular, and (c) inverse profiles.

functions grouped around the most significant harmonic. In that case the N_1 members of sum (13) are grouped around the frequency on which the product $F_m(\nu)F_l^*(\nu)$ has the maximum value, which is explained in more detail in [10]. In the examples treated in this paper the determination of these frequencies is simple. If we take $N_1 = 0$, then we get variant (10). It appears that the convergence regarding N_1 is very fast, so taking just a few of the nearest harmonics we obtain results almost identical with the results obtained when we take all N computed harmonics.

In [15] we found the ratio between the computation times of the original LSBRM and procedure (12) to be

$$T = \frac{N_1}{N} + \frac{\log_2 N}{M} \tag{16}$$

where M is the number of modes (i.e., expansion coefficients), N is the number of function samples (FFT harmonics), and N_1 is the number of the most significant modes of sum (13).

In system (10) the summation applied in (13) is excluded (i.e., $N_1 = 0$) so the time ratio is now

$$T_0 = \frac{\log_2 N}{M}. \tag{17}$$

III. Application to Diffraction Problems

The applicability of this method using different numbers of harmonics (i.e., N_1) will be demonstrated on electromagnetic wave diffraction from periodic gratings of perfect conductivity. We shall consider the grating of the sinusoidal profile (Fig. 1(a)) which has very often been used as a testing profile [6], [16], [17] and also of the semicircular profile (Fig. 1(b) and (c)) used in [18].

As usual, we are assuming an incident plane wave of normal polarization:

$$E_i = E_0 e^{-jk(\gamma x - \delta z)} \tag{18}$$

with

$$\gamma = \sin\theta \qquad \delta = \cos\theta$$
$$k = 2\pi/\lambda \qquad E_0 = 1. \tag{19}$$

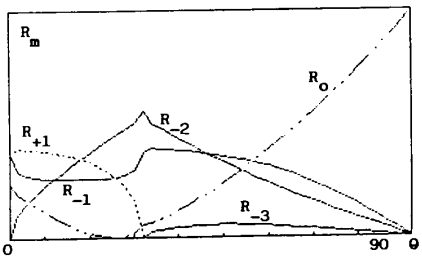

Fig. 2. The reflection coefficients in sinusoidal grating: $h/\lambda = 0.5$; $d/\lambda = 2$.

TABLE I
Energy Balance for Sinusoidal Grating

diffraction from sinusoidal grating
d/λ=2. h/λ=0.5 M=15

N1=31		N1=3		N1=0	
angle	energy sum	angle	energy sum	angle	energy sum
0	0.9999929	0	1.000010	0	0.9981373
10	0.9999952	10	1.000241	10	1.0007950
20	0.9999846	20	1.000772	20	0.9956011
30	0.9999901	30	1.000671	30	1.0000000
40	0.9999971	40	1.000107	40	1.0003840
50	0.9999933	50	1.000088	50	1.0018050
60	0.9999891	60	1.000021	60	1.0022290
70	0.9999902	70	1.000407	70	1.0003760
80	0.9999973	80	1.000104	80	0.9978624
89	0.9999979	89	1.000029	89	1.0005470

The reflected field is represented as a sum of propagating and attenuated waves:

$$E_r = \sum_{m=-M}^{M} E_m e^{-jk(\gamma_m x + \delta_m z)} \tag{20}$$

with

$$\gamma_m = \sin\theta + m\lambda/d \qquad \delta_m = \sqrt{1-\gamma_m^2}.$$

The unknown $2M+1$ coefficients E_m are determined by the previously described procedure satisfying the boundary condition on the grating wall:

$$E_r = E_i. \tag{21}$$

Thus, we have

$$f_m(x) = e^{-jk(\gamma_m x + \delta_m l(x))}$$
$$g(x) = -e^{-jk(\gamma x + \delta l(x))}. \tag{22}$$

Having found field amplitudes E_m we plotted the reflection coefficients against the incident angle:

$$R_m = |E_m|^2 \frac{\delta_m}{\delta}. \tag{23}$$

For a sinusoidal grating the reflection coefficients are shown in Fig. 2.

As an accuracy test energy conservation was employed:

$$\sum_m |E_m|^2 \frac{\delta_m}{\delta} = 1. \tag{24}$$

The summation went over those values of m for which δ_m was real. As can be seen from Table I the requirement imposed by (23) was rigorously satisfied.

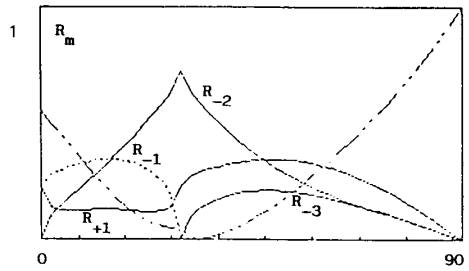

Fig. 3. The reflection coefficients in the case of semicircular grating: $h/\lambda = 0.5$; $d/\lambda = 2$.

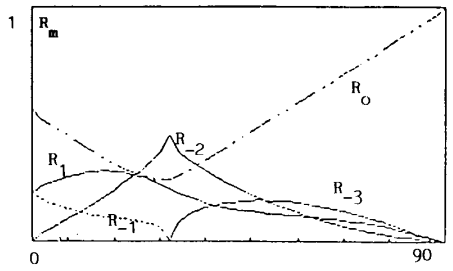

Fig. 4. The reflection coefficients in the case of inverse grating ($h/\lambda = 0.5$; $d/\lambda = 2$).

Here the error is less than 0.5 percent for $N_1 = 0$ and $N = 64$. For $N_1 = 31$ the error is even less than 0.002 percent. In the former, when $N_1 = 0$, the time ratio is 0.193 and for $N_1 = 31$ it is 0.678. So, by using system (10) we obtain the coefficients 5.18 times faster than by using the original LSBRM method. As can be seen, if we take just $N_1 = 3$ then the value of error is very close to that in $N_1 = 31$. However, when $N_1 = 3$, the computation is four times faster than in the original LSBRM procedure.

The fulfillment of the boundary condition (eq. (21)) can be used as another accuracy check. Although it is not presented here, this check has been performed and it has proved the high accuracy of the results.

We solved the diffraction problem of semicircular (Fig. 1(b)) and inverse (Fig. 1(c)) gratings in the same way. Incident wave and boundary data are the same as in the previous example. The reflection coefficients are shown in Figs. 3 and 4.

The energy balance for a semicircular grating is given in Table II. The error is less than 2 percent for a semicircular grating with $N_1 = 5$ and even less than 0.3 percent with $N_1 = 31$. This was achieved with $M = 15$, that is, with the 31 modes in (20) and with 256 samples along the grating wall, within the interval $(0, d)$. Taking $N_1 = 0$ we could not get acceptable results for all angles of incidence, so they are not given in Table II. The reason for this might be the existence of sharp edges in this structure.

For $N = 256$, $M = 31$, and $N_1 = 31$ the time ratio of performed calculations is 0.5, which means that the modified version of the LSBRM is approximately two times faster than the original method. With $N_1 = 5$, it is 3.5 times faster.

TABLE II
ENERGY BALANCE OF SEMICIRCULAR GRATING

diffraction from semicircular grating
d/λ=2. h/λ=0.5 M=15

N_1=5		N_1=31	
angle	energy sum	angle	energy sum
0	1.0047280	0	1.0021250
10	0.9908099	10	1.0006920
20	0.9837392	20	0.9970310
30	1.0181570	30	0.9975786
40	0.9955971	40	1.0004160
50	0.9827893	50	1.0007570
60	0.9863375	60	1.0020270
70	1.0016860	70	1.0028000
80	0.9929035	80	1.0022110
89	1.0012530	89	1.0005470

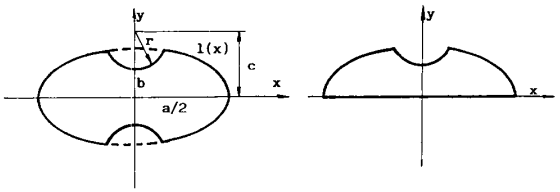

Fig. 5. A cross section of elliptical and ridged elliptical waveguides.

As was expected, in each of these cases rather pronounced Wood's anomalies were found at an angle of incidence of $\theta = 30°$. The reason for this is that a double grazing occurs ($|\gamma_m| = 1$), the grazing orders being -3 and $+1$. An especially strong coupling is among -2 and 0 orders and, since -2 is a backscattering wave, it suffers the strongest resonant effect, as was explained in detail in [19].

IV. The Eigenvalue Problems

As an illustration of the applicability of the suggested method in solving eigenvalue problems, we shall consider ridged elliptical waveguides (Fig. 5) with H wave.

Elliptical waveguides are often taken as a reference when comparing the numerical methods with analytical results [20], [21]. Assuming that the volume is the same, conventional elliptical waveguides, as is known [22], have a lower attenuation factor than circular and rectangular ones. We shall examine the characteristics of ridged elliptical waveguides which, as will be shown, have a lower cutoff frequency and a wider bandwidth but a greater attenuation factor.

The differential equation for the longitudinal magnetic field component $U = H_z$ is the same as (1), and the boundary condition on the waveguide walls is

$$\frac{\partial Hz}{\partial n} = 0 \tag{25}$$

so system (12) becomes

$$\begin{Vmatrix} A_{11} & \cdots & A_{1M} \\ \vdots & & \vdots \\ A_{M1} & \cdots & A_{MM} \end{Vmatrix} \begin{Vmatrix} c_1 \\ \vdots \\ c_M \end{Vmatrix} = 0. \tag{26}$$

TABLE III
NORMALIZED EIGENVALUE $k/(2/a)$ OF H_{11}^c MODE OF ELLIPTICAL AND RIDGED ELLIPTICAL WAVEGUIDES ($a=1$, $b=0.6$, $M=11$, $N=64$)

ELLIPTICAL			RIDGED ELLIPTICAL			
			r=0.3 c=0.7		r=0.3 c=0.6	
analytic	*	**	*	**	*	**
1.868	1.868	1.868	1.696	1.696	1.560	1.587

results obtained by: * - system (10) ** - system (15)

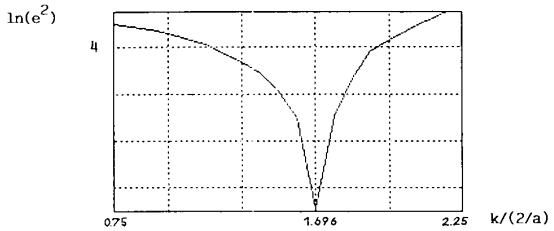

Fig. 6. The behavior of e^2 against $k/(2/a)$ for elliptical waveguide where $a=2$ and $b=0.6$.

We shall assume H_z for the H_{11}^c mode to be

$$H_{z11}^c = \sum_{m=1}^{M} c_m \sin\frac{(2m-1)\pi x}{a}\cos k_y y$$

$$k_y^2 + \left[\frac{(2m-1)\pi}{a}\right]^2 = k^2. \tag{27}$$

The superscript c indicates the H_{11} mode odd with respect to the longer ellipse axis.

The nontriviality condition for system (26) requires

$$\det\|A_{mn}\| = 0 \tag{28}$$

where $A_{mn} = A_{mn}(k)$. For different values of the relative eigenvalue $k_r = k/(2/a)$ we shall calculate $\det\|A_{mn}\|$. The unknown eigenvalues are those values for which the determinant reaches the minimum. However, as in [15], we achieved better results by taking $c_1 = 1$, finding the integral of the absolute square error e, and then coefficients c from (26). By changing the value of k_r, we found the minimum of e^2 and thus the eigenvalue we were seeking.

The eigenvalues for elliptical waveguides obtained by systems (10) and (12) are compared with analytically obtained eigenvalues in Table III. The behavior of the absolute square error integral using system (10) can be seen from Fig. 6.

For the ridged elliptical waveguides (Fig. 5) we also used the H_z approximation given by (27). Again, applying procedure (10) and procedure (12), we found the eigenvalues for two sets of ridge parameters. The results are given in the middle and right-hand columns of Table III. For a relatively shallow ridge the results are identical, but for a deeper ridge a slight difference appears.

It is interesting to see the distribution of error $e(x)$ around the boundary curve of the cross section. This is shown in Fig. 7 for systems (10) and (12). They are close, but the peak value of error produced by system (10) is greater. It is also greater along most of the boundary line.

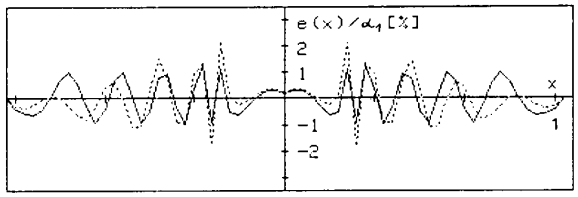

Fig. 7. Error along boundary line where $a=2$, $b=0.6$, $r=0.3$, and $c=0.7$.

TABLE IV
NORMALIZED EIGENVALUE $k/(2/a)$ OF H_{11}^s, H_{12}^c MODES OF THE RIDGED ELLIPTICAL WAVEGUIDE ($a=1$, $b=0.6$) FOR H_{11}^c ($M=11$, $N=64$); FOR H_{12}^c ($M=21$, $N=128$)

	ELLIPTICAL		RIDGED ELLIPTICAL	
	analytic		r=0.3 c=0.7	r=0.3 c=0.6
H_{11}^s	2.985	2.978	3.204	3.314
H_{12}^c	3.385	3.377	3.487	3.644

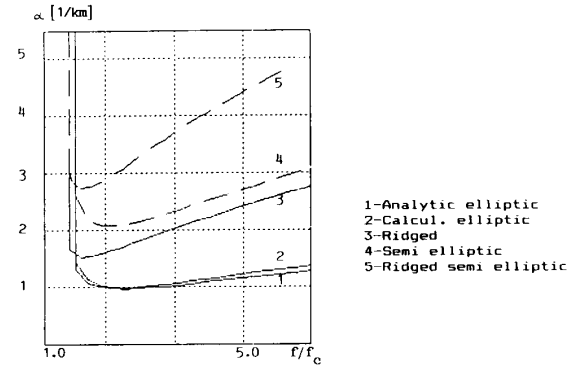

Fig. 8. Attenuation factor for H_{11}^c mode of elliptical (semielliptical) and ridged waveguide (with one and two ridges) with $a=1$, $b=0.6$, $c=0.6$, and $r=0.3$.

Therefore, using (10), we found eigenvalues for the H_{11}^s and H_{12}^c modes taking

$$H_{11}^s: \quad H_{z11}^s = \sum_{m=1}^{M} c_m \cos\frac{(2m-1)\pi}{a} x \sin k_y y$$

$$H_{12}^c: \quad H_{z12}^c = \sum_{m=1}^{M} c_m \cos\frac{2m\pi}{a} x \cos k_y y. \tag{29}$$

Superscript s indicates the H_{11} mode even with respect to the longer ellipse axis.

The results are given in Table IV. For the elliptical waveguides they are again compared with analytical results. The number of modes and samples is given below the table.

Having found the coefficients c_m, we can easily calculate the attenuation factors from the formula

$$\alpha = \frac{R_s \int_L |H_t|^2\, dl}{2\int_S |H_T|^2\, ds}, \qquad R_S = \sqrt{\frac{\pi\mu f}{\sigma}} \tag{30}$$

where all the other field components are derived from H_z

in the usual manner (H_T is the transversal cross-sectional component, H_t is the tangential boundary line component). They are given in Fig. 8, which also shows the analytically obtained attenuation factor for the elliptical waveguide (conductivity is taken to be $\sigma = 62.9\ 10^6$ [S/m]). As we can see the difference is small.

All calculations in this paper were carried out on a VAX = 11/780.

V. Conclusion

The original LSBRM was modified using FFT of the basis and boundary condition functions along the boundary. This approach led to numerical procedures that can be treated as special cases of the general moment method with FT of basis functions as weighting functions. Procedures differ by the number of FT harmonics, which ranges from complete FT to no more than one FT harmonic of basis functions along the boundary. The first possibility is equivalent to the requirement that the mean square absolute error is minimum, while the second possibility actually leads to an improved collocation procedure.

In several diffraction and eigenvalue problems treated in this paper we found that, in order to obtain very accurate results, it was sufficient to take just a few (three to five) FT's of the mainly contributing harmonics of the basis functions. Consequently, this resulted in substantial saving in computation time compared to the original LSBRM.

References

[1] F. F. Cap, "Boundary values problems of unseparable linear partial differential equation," *Z. Angew. Math. Mech.*, vol. 66, no. 6, 1986.

[2] F. L. Ng, "Tabulation of methods for numerical solution of hollow waveguide problem," *IEEE Trans. Microwave Theory Tech.*, vol. MTT-22, Mar. 1974.

[3] S. M. Saad, "Review of numerical methods for the analysis of arbitrarily shaped microwave and optical dielectric waveguides," *IEEE Trans. Microwave Theory Tech.*, vol. MTT-33, Oct. 1985.

[4] L. Lewin, "On the inadequacy of discrete mode-matching techniques in some waveguide discontinuity problems," *IEEE Trans. Microwave Theory Tech.*, vol. MTT-18, May 1972.

[5] R. F. Millar, "On the Rayleigh assumption in scattering by periodic surface," *Proc. Cambridge Phil. Soc.*, vol. 69, 1971.

[6] H. Ikuno and K. Yasuura, "Improved point-matching method with application to scattering from periodic surface," *IEEE Trans. Antennas Propagat.*, vol. AP-21, Sept. 1973.

[7] H. Lariviere and J. B. Davies, "The solution of electromagnetic eigenvalue problems by least-squares boundary residuals," *IEEE Trans. Microwave Theory Tech.*, vol. MTT-25, May 1975.

[8] J. Atechian,H. Baudrand, and J. Pahn, "Composite dielectric waveguide," *Electron. Lett.*, vol. 20, no. 4, pp. 189–190, Feb. 1984.

[9] J. B. Davies, "Surface acoustic wave propagation on a piezo-electric substrate with a periodic metal grating," *Electron. Lett.*, vol. 20, no. 18, pp. 720–722, Aug. 1984.

[10] S. Jovićević and LJ. Stanković, "The boundary condition expansion on basic function-application in electrostatics," in *Proc. XXX-th ETAN*, June 1986, pp. 187–194.

[11] LJ. Stankovic and S. Jovićević, "Determination of electromagnetic field distribution by boundary condition expansion on basic function," in *Proc. XXXI-th ETAN*, June 1987, pp. 135–142.

[12] LJ. Stanković and S. Jovićević, "A round ridge waveguide," *Ann. Telecommun.*, 43, nos. 9–10, Oct. 1988.

[13] H. Baudrand, M. Boussouis, and J. L. Amalric, "Analyses of some planar structures by the least-squares boundary residual method," *IEEE Trans. Microwave Theory Tech.*, vol. MTT-34, pp. 298–301, Feb. 1986.

[14] A. V. Oppenheim and R. W. Schafer, *Digital Signal Processing*. Engelwood Cliffs, NJ. Prentice-Hall, 1975.

[15] LJ. Stanković and S. Jovićević, "Modified least squares method with application in diffraction and eigenvalue problems," *Proc. Inst. Elec. Eng.*, vol. 135, part H, pp. 339–343, Oct. 1988.

[16] A. Wirgin, "Scattering from sinusoidal grating: An evoluation of the Kirchhoff approximation," *J. Opt. Soc. Amer.*, vol. 73, no. 8, Aug. 1983.

[17] G. Whitman and F. Schwering, "Scattering by periodic metal surfaces with sinusoidal height profiles—A theoretical approach," *IEEE Trans. Antennas Propagat.*, vol. AP-25, Nov. 1977.

[18] A. R. Panicali, "Radiation pattern synthesis techniques as applied to the study of perfectly conducting periodic structures of arbitrary profile: TE-polarization," *IEEE Trans. Antennas Propagat.*, vol. AP-25, May 1977.

[19] S. Jovićević and S. Sesnić, "Diffraction of a parallel and perpendicular-polarized wave from an echellete grating," *J. Opt. Soc. Amer.*, vol. 62, pp. 865–877, 1972.

[20] P. Daly, "Finite element approach to propagation in elliptical and parabolic waveguides," *Int. J. Numer. Meth. Eng.*, vol. 20, 1984.

[21] I. G. Kretzschmar, "Propagation in hollow elliptical waveguides," *IEEE Trans. Microwave Theory Tech.*, vol. MTT-18, Apr. 1970.

[22] I. E. Efimov and G. A. Sermina, *Volnovodie Linii Peredaci*. Moscow: *Svjaz*, 1979.

[23] R. F. Harrington, *Field Computation by Moment Methods*. New York: Macmillan, 1968.

[24] S. Jovićević and LJ. Stanković, "The wave diffraction from a strip grating," in *Proc. XXXII-th ETAN*, June 1988, pp. 189–196.

✠

Ljubiša Stanković was born 1960 in Montenegro, Yugoslavia. He received the B.S. degree from the University of Titograd (1982), the M.Sc. degree from the University of Belgrade (1984), and the Dr. technical Sc. degree from the University of Titograd (1988). In 1984 and 1985 he was at the Worcester Polytechnic Institute, Worcester, MA.

Currently he is an Assistant Professor of Digital Signal Processing in the Electrical Engineering Department of the University of Titograd. His main contributions are both in numerical methods of electromagnetic field computation and digital signal processing, in which field he recently published a book.

✠

Svetozar Jovićević was born 1942 in Montenegro, Yugoslavia. He received the B.S. degree from the University of Titograd (1965), the M.Sc. degree from the University of Belgrade (1969) and the Dr. technical Sc. degree from the University of Zagreb (1972). In 1972 he was at the University of Texas, Austin, and in the academic year 1977/1978 he did postdoctoral study at the University of Southampton, U.K.

As a Professor he teaches electromagnetic theory in the Electrical Engineering Department and the Department of Physics at the University of Titograd. His main contributions are in numerical methods of electromagnetic field computation.

Dr. Jovićević has served as Dean of the Electrical Engineering Department and Dean of Technical Faculty of the University of Titograd.